JPET Fast Forward. Published on December 20, 2005 as DOI: 10.1124/jpet.105.097618

Title Page

KN-93, a Calcium/Calmodulin-Dependent Protein Kinase II Inhibitor, is a Direct Extracellular Blocker of Voltage-Gated Potassium Channels

Saman Rezazadeh, Thomas W. Claydon and David Fedida

Department of Cellular and Physiological Sciences (S.R., T.W.C., D.F.)
University of British Columbia
Vancouver, British Columbia
V6T 1Z3, Canada

Running Title Page

Running title: KN-93 block of Kv Channels

Correspondence to: Dr. David Fedida,
Department of Cellular and Physiological Sciences,
2350 Health Sciences Mall, Vancouver B.C. V6T 1Z3
Canada
Tel: (604) 822-5806; FAX: (604) 822-6048;
E-mail: fedida@interchange.ubc.ca

Number of text pages: 27
Number of Tables: 0
Number of Figures: 6
Number of References: 25
Number of Words in Abstract: 234
Number of Words in Introduction: 482
Number of Words in Discussion: 809
Recommended Section Assignment: Neuropharmacology

List of non-standard abbreviations: CaMKII, Ca^{2+}/calmodulin-dependent protein kinase II; CIP, CaMK II inhibitory peptide fragment; HEK, human embryonic kidney; hERG, human ether a-go-go related gene; Kv, voltage-gated potassium channels; *G*, chord conductance; IC_{50}, the concentration required to achieve half maximal block; *k*, slope factor; $V_{1/2}$, half-activation potential.

Abstract

The effect of Ca^{2+}/calmodulin-dependent protein kinase II (CaMK II) on voltage-gated ion channels is widely studied through the use of specific CaMK II blockers such as KN-93. The present study demonstrates that KN-93 is a direct extracellular blocker of a wide range of cloned Kv channels from a number of different subfamilies. In all channels tested, the effect of 1 μM KN-93 was independent of CaMK II since 1 μM KN-92, an inactive analog of KN-93, caused similar inhibition of currents. In addition, dialysis of cells with 10 μM CaMK II inhibitory peptide fragment 281-301 (CIP), had no effect on current kinetics and did not prevent the inhibitory effect of KN-93. The IC_{50} for block of the Kv1.5 channel (used as an example to determine the nature of KN-93 block) was 307 ± 12 nM. KN-93 blocked open channels with little voltage-dependence that did not alter the $V_{1/2}$ of channel activation. Removal of P/C-type inactivation by mutation of arginine 487 to valine in the outer pore region of Kv1.5 (R487V) greatly reduced KN-93 block, while enhancement of inactivation induced by mutation of threonine 462 to cysteine (T462C) increased the potency of KN-93 by four-fold. This suggested that KN-93 acted through promotion and stabilization of C-type inactivation. Importantly, KN-93 was ineffective as a blocker when applied intracellularly, suggesting that CaMK II-independent effects of KN-93 on Kv channels can be circumvented by intracellular application of KN-93.

Introduction

Voltage-gated potassium (Kv) channels, which are activated by changes in the transmembrane potential, play an important role in the control of excitability. There are a number of structurally related sub-families of Kv channels (Chandy 1991) that are expressed in a wide range of tissues, such as heart (e.g. Kv1, Kv2, Kv4 and hERG), brain (Kv1, Kv2, Kv3 and Kv4), pancreas and smooth muscle (e.g. Kv1) (Shieh et al., 2000). It is well documented that Kv channels are crucial targets for protein kinase activation and that phosphorylation can affect channel characteristics (Levitan, 1994). Calcium/calmodulin kinase II (CaMK II) is a multi-functional cytoplasmic calcium and calmodulin-dependent protein kinase that phosphorylates and alters the function of a variety of substrates. Given that members of a number of Kv channel subfamilies are expressed in the brain (Shieh *et al.*, 2000) and the abundance of expression of CaMK II in the brain (Braun and Schulman, 1995), it comes as no surprise that CaMK II has been suggested to phosphorylate Kv channels (Roeper *et al.*, 1997). Roeper *et al.* (1997) showed that the rate of fast N-type inactivation of the *Shaker* related Kv1.4 channel is modulated by CaMKII phosphorylation of serine 123 in the N-terminus. Similarly, the rate of fast inactivation of Kv4.3 was recently shown to be slowed by CaMK II phosphorylation of serine 550 in the C-terminus (Sergeant *et al.*, 2005). In addition to these effects on channel gating, CaMK II also increased surface expression of Kv4.2 and drosophila *ether a go-go* (*eag*) potassium channels (Wang *et al.*, 2002; Varga *et al.*, 2004; Sun *et al.*, 2004). The regulatory effect of CaMK II is not limited to potassium channels, since CaMK II has been shown to alter the activation properties of the sodium channel, $Na_V1.5$ (Young and Caldwell, 2005).

The effect of CaMK II on ion channel function has been widely studied through the use of specific inhibitors such as KN-93. KN-93 is a methoxybenzenesulfonamide compound, which

exerts its effect by competing for the calmodulin (CaM) binding site of CaMK II with an IC_{50} of 370 nM (Sumi *et al.*, 1991) and is an extensively used inhibitor of CaMK II. For example, inhibition of CaMK II with KN-93 incubation enhanced N-type inactivation of Kv1.4 and Kv4.3 (Roeper *et al.*, 1997; Sergeant *et al.*, 2005), an observation that is consistent with CaMK II induced slowing of inactivation. However, Ledoux *et al.* (1999) have shown that caution must be taken in the interpretation of such experiments since KN-93 affected Kv currents in rabbit portal vein smooth muscles independently of CaMK II action.

In the present study, we have extended these initial observations to show a direct effect of KN-93 on a wide range of cloned Kv channels heterologously expressed in mammalian cells is independent of CaMK II. KN-93 is a potent extracellular open channel blocker of all Kv channels tested and exerts its effect by enhancing C-type inactivation.

Methods

Materials Cell culture supplies were purchased from Invitrogen (Burlington, ON). KN-92 (2-[N-(4-Methoxybenzenesulfonyl)]amino-N-(4-chlorocinnamyl)-N-methylbenzylamine, Phosphate), KN-93 (2-[N-(2-hydroxyethyl)]-N-(4-methoxybenzenesulfonyl)]amino-N-(4-chlorocinnamyl)-N-methylbenzylamine) and the CaMK II inhibitory peptide fragment 281-301 (CIP) were obtained from Calbiochem (San Diego, CA). 5 mM stock solutions of KN compounds were made in 100% DMSO (Sigma, Mississauga, ON). The maximum final working concentration of DMSO was 0.06%, which had no effect on Kv channels tested (data not shown). CIP was reconstituted in distilled water as a 1 mM stock solution. All other chemical reagents used to make solutions were purchased from Sigma.

Cell Culture and Transfection Experiments were performed on HEK 293 cells either stably (human ether a-go-go related gene (hERG), Kv1.5, Kv1.5 R487V, Kv1.4 Δ 2-147 and Kv4.2) or transiently (Kv1.2, Kv2.1, Kv3.2 and all other Kv1.5 point mutations) expressing cloned channels. HEK 293 cells stably expressing channels were grown in minimum essential medium (MEM), 10 % fetal bovine serum (FBS), penicillin-streptomycin and 1 mg ml^{-1} gentamicin. Transient transfections were performed with HEK 293 cells plated at 20-30 % confluency on sterile coverslips in 25 mm Petri dishes one day prior to transfection. 2 μg of ion channel DNA was incubated with 1 μg of eGFP DNA (to enable detection of transfected cells) and 3 μl of lipofectamine 2000 (Invitrogen) in 100 μl of Opti-MEM and added to the cells after changing the media with 900 μl of MEM with 10 % FBS. All cells were maintained at 37 °C in an atmosphere of 5 % CO_2/air.

Molecular Biology and Channel Mutations The mammalian expression system pcDNA3.1 (Invitrogen) was used for expression of all constructs in this study. All point mutations in Kv1.5

were performed using the PCR-based QuickChange™ site-directed mutagenesis kit (Stratagene, San Diego, CA) using primers constructed by Sigma-Genosys (Oakville, ON). All constructs were sequenced at the University of British Columbia core facilities (Vancouver, BC) to ensure the fidelity of the PCR reactions.

Electrophysiology solutions For recording potassium current, the pipette solution contained (mM): KCl, 130; EGTA, 5; $MgCl_2$, 1; HEPES, 10; Na^+_2ATP, 4; GTP, 0.1 (adjusted to pH 7.2 with KOH). The bath solution contained (mM): KCl, 5; NaCl, 135; $MgCl_2$, 1; sodium acetate, 2.8; HEPES, 10 (adjusted to pH 7.4 with NaOH). High extracellular K^+ experiments were performed using bath solution containing (mM): KCl, 135; HEPES, 10; $MgCl_2$, 1; Dextrose, 10 (adjusted to pH 7.4 with KOH). For recording currents through Kv1.5 R487V, the pipette solution contained (mM): NaCl, 130; Na^+_2ATP, 4; $MgCl_2$, 1; HEPES, 5; EGTA, 10; GTP, 0.1 (pH adjusted to 7.2 with NaOH). The bath solution contained (mM): NaCl, 5; NMDG, 130; HEPES, 10; Dextrose, 10; $MgCl_2$, 1 (pH adjusted to 7.4 with HCl). KN compounds were diluted in bath solution at the appropriate concentration immediately prior to each experiment and kept in the dark, in order to avoid photo destruction of the drug. For experiments with CIP and internal KN-93, the compounds were diluted in pipette solution at the appropriate concentration.

Electrophysiological Procedures Glass coverslips to which cells were adhered were removed from the incubator immediately prior to experiments and placed in a recording chamber mounted on the stage of an inverted phase contrast microscope at room temperature. The bath solution was constantly flowing. Patch electrodes fashioned from thin-walled borosilicate glass (World Precision Instruments, FL, USA) had a resistance of 1.5-2.5 MΩ when filled with the pipette solution. Whole-cell current recording and data analysis were performed using an Axopatch 200B amplifier, DigiData 1322A digitizer and pClamp8 software (Axon instruments, Foster

City, CA). Capacity compensation and 80% serial resistance compensation were used in all whole-cell recordings. Data were sampled at 10 kHz and filtered at 2 kHz. No leak subtraction was used and dashed lines on current records represent the zero current level.

Data Analysis Potency of each drug was determined by fitting the concentration-response relationships with the Hill equation (1) using GraphPad Prism 3.02 (San Diego, CA):

$$y=1/(1+(IC_{50}/[\text{KN-93}])^{n}) \quad (1)$$

where y is the fraction of current remaining at a given membrane potential, IC_{50} is the concentration required to achieve half maximal block, [KN-93] is the concentration of KN-93 in the bath solution, and n is the Hill coefficient. Chord conductance (G) at a given potential was calculated by dividing the current at the end of a 300 ms pulse by the driving force calculated from the Nernst equation. G-V curves were fitted with a single Boltzmann function:

$$y=1/(1 + \exp[(V_{1/2} - \text{V})/k]) \quad (2)$$

where y is the conductance normalized with respect to the maximal conductance, $V_{1/2}$ is the half-activation potential, V is the test voltage and k is the slope factor.

The pore structure of Kv1.5 was modeled using the known crystal structure of the related Kv1.2 channel (accession: 2A79) as a template using Swiss-Model's "First Approach Mode" (**http://swissmodel.expasy.org/SM_FIRST.html**) and "Swiss-Pdbviewer". Data throughout the text and figures are shown as means ± S.E.M. Statistical significance was determined throughout using Student's *t* test with P values of less than 0.05 taken to be significant.

Results

KN-93 inhibits a wide range of Kv channels. Given the initial observations of Ledoux *et al.* (1999) in rabbit portal vein smooth muscle, where the types of Kv channels directly affected by KN-93 were not identified, we examined the effect of KN-93 on a range of Kv channel representatives from a number of different subfamilies. Figure 1A shows typical current traces recorded from Kv1.2, Kv1.5, Kv1.4 Δ2-147, Kv2.1, Kv3.2, Kv4.2 and hERG channels during perfusion of control solution or solution containing 1 μM KN-93. Kv1.4 Δ2-147 was used to remove fast inactivation from the channels and reveal any effect of KN-93. Currents were recorded during voltage pulses to +60 mV for 5 s every 40 s with the exception of Kv4.2 currents, which were recorded during 200 ms pulses every 10 s and hERG currents, which were recorded during 4 s pulses to –50 mV following a 4 s pulse to +20 mV. In all channels tested, KN-93 enhanced current decay so that the current amplitude at the end of the pulse was significantly reduced (Fig. 1B, filled bars). In some channels, KN-93 also inhibited the peak current (e.g. Kv1.2, Kv2.1 in Fig. 1A), but this was probably due to the slower activation kinetics of these channels (as shown by the scaled traces) rather than any additional effect of KN-93 on these channels. To demonstrate that the effect of KN-93 on Kv channels was independent of CaMK II, we repeated these experiments using KN-92, the inactive, but structurally very similar, form of KN-93. The open bars in Fig. 1B show that, like KN-93, KN-92 significantly reduced the sustained current amplitudes at the end of the 5 s depolarizing pulses of all channels tested. These data show that KN-93 inhibits a wide range of Kv channels in a manner that is independent of CaMK II.

KN-93 directly blocks the Kv1.5 channel. Since Kv1.5 is thought to be the major constituent of the delayed rectifier current in the rabbit portal vein smooth muscle cells (Overturf *et al.*,

1994) and KN-93 has been shown to act as a direct blocker of Kv currents in these cells (Ledoux *et al.*, 1999), we used Kv1.5 to examine the nature of the KN-93 inhibition of Kv currents. Data in Fig. 2A shows typical traces recorded from Kv1.5 channels in the presence of a number of different concentrations of KN-93. The current amplitude at the end of the 5 s pulse at each concentration was used to construct the concentration-response curve shown in Fig. 2B. A non-linear least-squares fit of the Hill equation to the concentration-response data yielded an IC_{50} value of 307 ± 12 nM and a Hill coefficient, *n*, of 1.3 ± 0.3 (Fig. 2B).

In order to rule out the involvement of CaMK II inhibition by KN-93 in the observed inhibition of Kv current, we used the CaMK II inhibitor peptide (CIP), a 29-amino-acid peptide corresponding to the CaM-binding domain of CaMK II. Dialysis of cells with 10 μM of CIP for 5 min had no effect on peak or sustained current amplitudes; after CIP treatment, average peak and sustained currents were 90 ± 3 % and 91 ± 5 % of the control pretreated value (n=5, Paired *t* test, not significant). A typical example is shown in the diary plot of Kv1.5 sustained current in Fig. 2C. Furthermore, inhibition of CaMK II with CIP did not prevent KN-93 from exerting its effect as demonstrated by the reduction of sustained current upon application of KN-93 to a value similar to that of cells not dialyzed with CIP; KN-93 inhibited current by 88± 2 % in the presence of CIP compared with 87 ± 2 % in the absence of CIP (Fig.2C; n=5, *t* test, not significant). These data are consistent with the observation that the inactive inhibitor, KN-92, induced a similar inhibition of sustained current to KN-93 (Fig. 1B).

In Fig. 3 the effect of KN-93 on the voltage-dependence of Kv1.5 channel activation was examined. Fig. 3A shows currents recorded during 300 ms pulses from –60 mV to +60 mV (in 10 mV increments) from a holding potential of –80 mV in the absence and presence of 1 μM KN-93. Conductance-voltage curves (Fig. 3B) were generated by calculating the chord

conductance from the current amplitude at the end of each pulse. The data were fitted to a single Boltzmann function (see Eqn. (2) in Methods). The deviation from the Boltzmann fit seen at depolarized potentials most likely represents an artifact that arises from the calculation of conductance from the current at the end of the pulse. It was not possible to calculate conductance from tail currents in these experiments because KN-93 reduced tail currents to such an extent that it was not possible to obtain accurate measurements. Fig. 3B shows that KN-93 appeared to shift the voltage-dependence of channel opening to more hyperpolarizing potentials as reported for the sustained K^+ currents of rabbit portal vein smooth muscle cells (Ledoux *et al.*, 1999), however, the data in did not reach statistical significance. The $V_{1/2}$ of activation was –7.7 ± 1.0 mV during control conditions and –12.8 ± 3.0 mV during perfusion of 1 μM KN-93. KN-93 did result in a significant decrease in the Boltzmann constant, *k*, from 8.6 ± 0.7 mV during control conditions to 4.8 ± 0.3 mV. Note that in Fig. 3A on the first pulse following channel opening at –20 mV, there is no apparent block due to KN-93. From data such as those recorded in Fig. 3A, we measured the degree of channel block in the presence of different concentrations of KN-93 over a range of potentials where the probability of channel opening was close to 1 ($V_m \geq 10$ mV) to construct concentration-response curves at each potential (Fig. 3C). The inset of Fig. 3C shows the dependence of the IC_{50} on membrane potential and highlights that KN-93 is only a weakly voltage-dependent blocker of Kv1.5.

KN-93 is an extracellular open-channel blocker of Kv1.5 channels. To examine the state dependence of accessibility of KN-93, a control current trace was recorded (Fig. 4A, left) and then 1 μM KN-93 was added to the bath while channels were held in the closed state (-80 mV) (Fig. 4A). The peak current obtained on the first opening of the channels following the 3 min incubation was not different from that of control; the average peak current on the first pulse

following a 3 min rest was 96 ± 2 % that of the control value (n=6, Paired *t* test, not significant). There was however, a pronounced effect on the peak current during the second depolarizing pulse, suggesting that KN-93 could not access its binding site in the closed state of the channel. We further examined the open state-dependent binding of KN-93 by inspecting the tail currents (Fig. 4B). Currents were recorded during 200 ms pulses to allow KN-93 binding before a hyperpolarizing pulse to –80 mV to observe tail currents. These experiments were performed in symmetrical K^+ conditions to increase tail current amplitude and therefore aid analysis. Tail currents obtained from the same cell in control conditions and in the presence of 1 μM KN-93 are shown in Fig. 4B. The tail currents were fitted to a double exponential function, which show that KN-93 significantly slowed the slow component of the tail current (mean time constant, τ_2, slowed from 52 ± 8 to 77 ± 5 ms, n=5; Paired *t*-test, $p<0.05$) causing the tail currents to crossover, a phenomenon that suggests that KN-93 is an open channel blocker that must unbind before the channel can close.

To identify which side of the membrane KN-93 exerts its effect, we dialyzed the cells with intracellular solution containing 1 μM KN-93 for 5 min after formation of the whole-cell configuration. Constant drug-free bath perfusion was maintained throughout. Cells were held at –80 mV and pulsed to +60 mV every 40 s for 5 min to document the effect of intracellularly applied KN-93. Fig. 4C and D show typical traces and a diary plot from such an experiment. It is clear, that at the end of the 5 min period with KN-93 applied intracellularly, sustained currents were not different from that obtained immediately after formation of whole-cell (Fig. 4C). To the same cell, we then applied KN-93 extracellularly by bath perfusion. Both Fig. 4C and D document that addition of KN-93 to the extracellular solution caused a rapid reduction of

sustained currents. These data suggest that KN-93 induces its effect from the extracellular side and is ineffective as a blocker from the intracellular solution.

Since nearly all known blockers of hERG involve drug binding at a site located in the central cavity of the pore (Mitcheson et al., 2000) we were interested to know whether KN-93 was an extracellular block of hERG as it is in Kv1.5. Fig. 4E and F show that hERG currents were not affected following a 5 min period with KN-93 applied intracellularly (n=3, Paired *t* test, not significant). In contrast, external KN-93 dramatically reduced hERG currents. These data suggest that KN-93 does not act by binding at the "classical" internal drug binding site of the hERG channel.

KN-93 delays recovery from inactivation. Data in Fig. 1 shows that Kv1.5 channels activate rapidly upon depolarization and then undergo slow inactivation over the course of a number of seconds, which results in the decay of the current while depolarization is sustained. Slow inactivation is thought to be caused by a local conformational change in the outer pore (P-type inactivation) followed by an energetically and structurally more complete stabilization of the inactivated conformation (C-type inactivation) (DeBiasi *et al.*, 1993; Loots and Isacoff, 1998; Kurata and Fedida, 2005). We measured the rate of recovery of Kv1.5 channels from inactivation in the absence (Fig. 5A) and presence of 1 μM KN-93 (Fig. 5B) by applying a +60 mV conditioning pulse for 5 s followed by brief (10 ms) test pulses to +60 mV applied at increasing intervals. The peak current amplitude obtained during each test pulse was normalized to that obtained during the conditioning pulse and plotted against the interpulse interval (Fig. 5C). The data points were fitted to a double exponential function, to represent recovery from P-type inactivation (τ_{fast}) and the more stable C-type inactivation (τ_{slow}). The data show that KN-93 slowed the fast phase of recovery from 255 ± 28 ms to 546 ± 61 ms (n=5; Paired t test, $p<0.05$)

and increased its contribution a_{fast} from 0.13 ± 0.04 to 0.32 ± 0.09 of the total inactivation (n=5; Paired *t*-test, $p<0.05$). KN-93 had no effect on the slow component of recovery from inactivation (n=5; Paired *t*-test, p =N.S.).

These results showed that inactivation was deeper and recovery from inactivation was delayed in the presence of KN-93 suggesting that KN-93 might interact with residues that regulate P-type inactivation in Kv1.5 and stabilize channels in the inactivated state. Given our data (Fig. 4) demonstrating extracellular binding of KN-93, we focused on extracellular residues known to be near the site of constriction responsible for inactivation and examined the effect of KN-93 on mutated Kv1.5 channels that showed reduced or accelerated slow inactivation. Data in Figure 6A shows currents recorded during a 1 sec depolarizing pulse to +60 mV from mutant channels in which the arginine at position 487 in the outer pore was replaced with a valine (R487V) (this is equivalent to the T499V mutation in *Shaker* (Lopez-Barneo *et al.*, 1993; Wang *et al.*, 2000). R487V mutant channels showed little inactivation during the pulse and the effect of 1 μM KN-93 was significantly reduced (Fig. 6A). Fig. 6B shows a model of the primary sequence of the Kv1.5 outer pore, based on that of the recently crystallized structure of the Kv1.2 channel (Long *et al.*, 2005), and reveals that the outer vestibule of the Kv1.5 pore is formed by the extracellular loops between the fifth and sixth transmembrane helices (S5-P-S6) and R487 is positioned close to the external mouth of the pore. In contrast to the R487V mutation, mutation of threonine 462 to cysteine (T462C) in the outer pore of the channel (Fig. 6B) resulted in an increased rate of inactivation (Fig. 6C). T462C currents inactivated so rapidly that currents were recorded during much shorter pulses; during a 500 ms depolarizing pulse to +60 mV, inactivation was comparable to that in the wild-type channel following a 5 s depolarization (Fig. 1B). Enhancement of inactivation by the T462C mutant was accompanied by increased block upon

exposure to KN-93 (Fig. 6C). Concentration-response curves generated using T462C current amplitudes at the end of the 500 ms depolarizing pulses in (Fig. 6D) show that the IC_{50} of block was significantly reduced to 69 ± 18 nM (n=4; P<0.05, Paired *t*-test, compared with wild-type). To test the correlation between KN-93 potency and outer pore mediated inactivation, we mutated each residue with the pore lining region of the outer vestibule (residues highlighted in Fig. 6B) and assessed the effect of KN-93. Of the eight mutations made, four were non-functional. However, H463C, S465C, S466C and P468C showed robust currents and these showed similar inactivation kinetics to the wild-type channel. The bar graph in Fig. 6E shows the effect of all of the mutations tested on the fractional current, normalized to control, remaining at the end of the pulse following KN-93 block. In contrast to the R487V and T462C mutations, which alter inactivation, the pore mutations that did not alter inactivation (H463C, S465C, S466C and P468C) showed a level of block that was not significantly different from control.

Discussion

KN-93 Inhibits a Wide Variety of Voltage-Gated Potassium Channels This study has demonstrated, for the first time, the direct interaction of KN-93, a specific CaMK II Inhibitor, with members of Kv1, Kv2, Kv3, Kv4, and Kv7 (hERG) voltage-gated potassium channel families. The effect of KN-93 on Kv channels was shown to be independent of CaMK II as 1) KN-92, an inactive form of KN-93, resulted in a similar inhibition of ionic currents (Fig. 1B), 2) dialysis of cells with CIP resulted in no detectable change in Kv1.5 currents or gating kinetics (Fig. 2C) and 3) Internal KN-93 did not alter channel gating (Fig. 4C and D). A number of lines of evidence suggest that KN-93 has a direct action as an open channel blocker of the Kv1.5 channel. Firstly, the currents shown in Fig. 3A and B recorded from the same cell in the absence and presence of KN-93 show that there was no block evident in the presence of the drug on the first pulse following channel opening (note the -20 mV traces). Secondly, incubation of cells held in the closed state with 1 μM KN-93 for 3 min resulted in no detectable effect on the peak current amplitude on the first depolarizing pulse (Fig. 4A). These results indicate that KN-93 cannot access its binding site when the channel is in the closed state. Finally, superposition of the tail currents in the presence and absence of KN-93 shows crossover (Fig. 4B), which suggests that channel closure is slowed by KN-93 unbinding from the open channel.

KN-93 stabilizes the inactivated state. Here, we have shown that KN-93 induces a rapid decay of current, and a reduction of peak current that is dependent upon the ability of the channel to inactivate. Reduction of the rate of inactivation, as in the Kv1.5 R487V mutation, markedly attenuated the effect of KN-93 (Fig. 6A). This suggests that KN-93 binding to open, and/or inactivated channels promotes the transition of channels to the inactivated state, and stabilizes them there. Consistent with this, recovery of channels from inactivation was slowed in the

presence of KN-93 (Fig. 5). Since the data in Fig. 6 suggest that KN-93 binds with a lower affinity to channels that inactivate slowly (e.g. R487V) this suggests that the concentration-response curve of R487V channels is right-shifted and we therefore expect that higher concentrations of KN-93 would induce greater block of R487V. Interestingly, we observed enhanced inactivation of Kv1.4 even in the absence of the N-terminus and therefore N-type inactivation (Fig. 1A), suggesting that at least part of the decay of current observed in Kv1.4 by Roeper *et al.* (1997) is due to a direct effect of KN-93 on slow inactivation of the channel. Enhancement of inactivation by the mutation Kv1.5 T462C in the outer pore enhanced the potency of KN-93 action (Fig. 6C and D). This increased block was unlikely to be due to allosteric effects on the outer pore structure because mutation of neighboring residues had no effect on either the rate of inactivation or the potency of KN-93 binding (Fig. 6E). Given that KN-93 acts at the extracellular side of membrane and interacts with the open channel (Fig. 4) and that the drug slows the recovery from the P-type inactivated state (Fig. 5), which involves reconfiguration of the outer pore, these results are consistent with the conclusion that, following open channel block, KN-93 promotes and stabilizes outer pore-dependent inactivation.

As a precedent for such an action, it is well documented that drug binding to hERG channel requires channel opening (Trudeau *et al.*, 1995; Zhou *et al.*, 1998), and there is a developing body of evidence suggesting that the block for most drugs occur via the inactivated state of the channel (Ficker *et al.*, 1998; Mitcheson *et al.*, 2000). Molecular determinants of high-affinity hERG block by a wide range of agents has been attributed to two aromatic residues in the S6 domain (Mitcheson *et al.*, 2000). It has been suggested that through inactivation, these two aromatic residues undergo a rotation and become exposed for drug block (Chen *et al.*, 2002). Since inactivation of Kv channels involves a physical conformational change in the outer pore

(Liu *et al.*, 1996) a similar mechanism may provide a favorable binding site for KN-93 in these channels.

In conclusion, the CaMK II inhibitor KN-93 and its inactive form, KN-92, inhibit a wide range of Kv channels. The present study shows that KN-93 is an external open channel blocker that shows little voltage-dependence and exerts its action by enhancement of inactivation. Since KN-93 is a potent blocker of many Kv channels, it must be used with caution. However, since KN-93 had no effect on Kv1.5 when applied intracellularly, CaMK II-independent effects of KN-93 on Kv channels can probably be circumvented by its intracellular application, although this should be confirmed for each channel system in which it is used.

Acknowledgements

We thank Ka-Kee Chiu for preparation of cells, and Cyrus Eduljee for the Kv1.5 T462C mutation.

References

Braun AP and Schulman H (1995) The multifunctional calcium/calmodulin-dependent protein kinase: from form to function. *Annu Rev Physiol* 57:417-445.

Chandy KG (1991) Simplified gene nomenclature. *Nature* 352:26.

Chen J, Seebohm G, and Sanguinetti MC (2002) Position of aromatic residues in the S6 domain, not inactivation, dictates cisapride sensitivity of HERG and eag potassium channels. *Proc Natl Acad Sci U S A* 99:12461-12466.

DeBiasi M, Hartmann HA, Drewe JA, Taglialatela M, Brown AM, and Kirsch GE (1993) Inactivation determined by a single site in K^+ pores. *Pflugers Arch* 422:354-363.

Ficker E, Jarolimek W, Kiehn J, Baumann A, and Brown AM (1998) Molecular determinants of dofetilide block of HERG K^+ channels. *Circ Res* 82:386-395.

Kurata HT and Fedida D (2005) A structural interpretation of voltage-gated potassium channel inactivation. *Prog Biophys Molec Biol* in press.

Ledoux J, Chartier D, and Leblanc N (1999) Inhibitors of calmodulin-dependent protein kinase are nonspecific blockers of voltage-dependent K^+ channels in vascular myocytes. *J Pharmacol Exp Ther* 290:1165-1174.

Levitan IB (1994) Modulation of ion channels by protein phosphorylation and dephosphorylation. *Annu Rev Physiol* 56:193-212.

Liu Y, Jurman ME, and Yellen G (1996) Dynamic rearrangement of the outer mouth of a K^+ channel during gating. *Neuron* 16:859-867.

Long SB, Campbell EB, and MacKinnon R (2005) Crystal structure of a mammalian voltage-dependent Shaker family K^+ channel. *Science* 309:897-903.

Loots E and Isacoff EY (1998) Protein rearrangements underlying slow inactivation of the *Shaker* K^+ channel. *J Gen Physiol* 112:377-389.

Lopez-Barneo J, Hoshi T, Heinemann SH, and Aldrich RW (1993) Effects of external cations and mutations in the pore region on C-type inactivation of Shaker potassium channels. *Recept Channels* 1:61-71.

Mitcheson JS, Chen J, Lin M, Culberson C, and Sanguinetti MC (2000) A structural basis for drug-induced long QT syndrome. *Proc Natl Acad Sci USA* 97:12329-12333.

Overturf KE, Russell SN, Carl A, Vogalis F, Hart PJ, Hume JR, Sanders KM, and Horowitz B (1994) Cloning and characterization of a $K_v1.5$ delayed rectifier K^+ channel from vascular and visceral smooth muscles. *Am J Physiol Cell Physiol* 267:C1231-C1238.

Roeper J, Lorra C, and Pongs O (1997) Frequency-dependent inactivation of mammalian A-type K^+ channel $K_V1.4$ regulated by Ca^{2+}/calmodulin-dependent protein kinase. *J Neurosci* 17:3379-3391.

Sergeant GP, Ohya S, Reihill JA, Perrino BA, Amberg GC, Imaizumi Y, Horowitz B, Sanders KM, and Koh SD (2005) Regulation of Kv4.3 currents by Ca^{2+}/calmodulin-dependent protein kinase II. *Am J Physiol Cell Physiol* 288:C304-C313.

Shieh CC, Coghlan M, Sullivan JP, and Gopalakrishnan M (2000) Potassium channels: Molecular defects, diseases, and therapeutic opportunities. *Pharmacol Rev* 52:557-593.

Sumi M, Kiuchi K, Ishikawa T, Ishii A, Hagiwara M, Nagatsu T, and Hidaka H (1991) The newly synthesized selective Ca^{2+}/calmodulin dependent protein kinase II inhibitor KN-93 reduces dopamine contents in PC12h cells. *Biochem Biophys Res Commun* 181:968-975.

Sun XX, Hodge JJ, Zhou Y, Nguyen M, and Griffith LC (2004) The eag potassium channel binds and locally activates calcium/calmodulin-dependent protein kinase II. *J Biol Chem* 279:10206-10214.

Trudeau MC, Warmke JW, Ganetzky B, and Robertson GA (1995) HERG, a human inward rectifier in the voltage-gated potassium channel family. *Science* 269:92-95.

Varga AW, Yuan LL, Anderson AE, Schrader LA, Wu GY, Gatchel JR, Johnston D, and Sweatt JD (2004) Calcium-calmodulin-dependent kinase II modulates Kv4.2 channel expression and upregulates neuronal A-type potassium currents. *J Neurosci* 24:3643-3654.

Wang Z, Wilson GF, and Griffith LC (2002) Calcium/calmodulin-dependent protein kinase II phosphorylates and regulates the Drosophila eag potassium channel. *J Biol Chem* 277:24022-24029.

Wang ZR, Hesketh JC, and Fedida D (2000) A high-Na^+ conduction state during recovery from inactivation in the K^+ channel Kv1.5. *Biophys J* 79:2416-2433.

Young KA and Caldwell JH (2005) Modulation of skeletal and cardiac voltage-gated sodium channels by calmodulin. *J Physiol* 565:349-370.

Zhou ZF, Gong QM, Ye B, Fan Z, Makielski JC, Robertson GA, and January CT (1998) Properties of HERG channels stably expressed in HEK 293 cells studied at physiological temperature. *Biophys J* 74:230-241.

Footnotes

This work was supported by grants from the Heart and Stroke Foundations of British Columbia and Yukon and the CIHR to D.F. S.R. was supported by University of British Columbia Graduate Fellowship. T.W.C was supported by postdoctoral research fellowship funded by a Focus on Stroke strategic initiative from The Canadian Stroke Network, the Heart and Stroke Foundation, the CIHR Institute of Circulatory and Respiratory Health and the CIHR/Rx&D Program along with AstraZeneca Canada.

Correspondence to: Dr. David Fedida,
Department of Cellular and Physiological Sciences,
2350 Health Sciences Mall, Vancouver B.C. V6T 1Z3
Canada
Tel: (604) 822-5806; FAX: (604) 822-6048;
E-mail: fedida@interchange.ubc.ca

S.R. and T.W.C contributed equally to this work.

Legends for Figures

Figure 1. KN-93 inhibits Kv channels from a number of different subfamilies. (A) Effect of 1 μM KN-93 on Kv1.2, Kv1.5, Kv1.4 Δ2-147, Kv2.1, Kv3.2, Kv4.2 and hERG currents. All currents were recorded during 5 s depolarizing pulses to +60 mV from a holding potential of –80 mV, in the presence and absence of 1 μM KN-93, with the exception of Kv4.2 (200 ms pulses to +60 mV) and hERG (4 s depolarization to +20 mV followed by a 4 s pulse to –50 mV to record tail currents). The pulse interval was 30 s for Kv4.2 and 40 s for all other channels in order to prevent cumulative inactivation. Gray lines depict current traces obtained in the presence of KN-93 scaled to the peak of the current in the absence of KN-93 to illustrate the effect of KN-93 on current decay. In case of Kv1.2 and Kv2.1, the slow activation results in normalized block to be underestimated (B) Summary of current inhibition by 1 μM KN-93 (filled bars) and the inactive form of KN-93, KN-92 (open bars). Fractional sustained current refers to the current at the end of the depolarizing pulse in the presence of drug normalized to the control value, with the exception of hERG currents, where peak tail currents in the presence of drug were normalized to those in the absence of drug. Numbers above bars represent n values. Significantly different from control: *, $P<0.05$; **, $P<0.01$ (Paired *t* test).

Figure 2. KN-93 inhibition of Kv1.5 is independent of CaMK II activity. (A) Kv1.5 currents recorded during 5 s pulses to +60 mV in the presence of increasing bath concentrations of KN-93. (B) Concentration-response curve for the effect of KN-93 on Kv1.5, from data such as those in (A). Data were fitted to a Hill equation (see Methods). The IC_{50} and Hill coefficient (*n*) are shown (n=4). (C) Diary of sustained current amplitude measured at the end of 5 s depolarizing pulses to +60 mV. Dialysis of cells with 10 μM CaMK II inhibitory peptide fragment 281-301

(CIP) is indicated by the broken line, and addition of KN-93 to the same cell by the first continuous line. Note that only KN-93 addition reduced sustained current amplitude.

Figure 3. Voltage-dependence of KN-93 effect. (A) Kv1.5 currents recorded in the absence (left) and presence (right) of 1 μM KN-93 during 300 ms pulses from –60 mV to +60 mV in 10 mV increments followed by a 200 ms pulse to –50 mV to measure tail currents. (B) Normalized conductance-voltage relationships in the absence and presence of 1 μM KN-93 determined based on the conductance at the end of each depolarizing pulse. Data were fitted to a single Boltzmann function. The $V_{1/2}$ of activation was –7.7 ± 1.0 mV in control conditions and –12.8 ± 3.0 mV in the presence of 1 μM KN-93 (n=4; Paired t test, p>0.05). The Boltzmann constant, k, was 8.6 ± 0.7 mV and 4.8 ± 0.3 mV, respectively (n=4; Paired t test, p<0.05). (C) Voltage-dependence of KN-93 inhibition determined from data such as those recorded in (A) in the presence of increasing concentrations of KN-93. The inset shows IC_{50} values plotted against the membrane potential. Points were connected by a line to guide the eye.

Figure 4. Extracellular binding Site of KN-93. (A) After a depolarizing pulse to +60 mV for 100 ms, the cell was held in the closed state (-80 mV) while the bath was perfused with 1 μM KN-93. This was followed by depolarizing pulses every 10 s. (B) Tail currents recorded from Kv1.5 channels with high extracellular K^+ (135 mM) at –80 mV after a 200 ms depolarizing pulse to +60 mV in the presence and absence of KN-93. Crossover of the two tracings is indicated by the arrow. Tail currents were fitted by a double exponential function. In the absence and presence of 1 μM KN-93, the mean fast time constant (τ_1) was 6.7 ± 0.8 and 6.9 ± 0.8 ms, respectively (n=5; Paired t test, p>0.05) and the mean slow time constant (τ_2) was 52 ± 8 and 77 ± 5 ms, respectively (n=5; Paired t test, p<0.05). The fractional amplitudes a_1 and a_2 were 0.91 ± 0.01 and 0.78 ± 0.01 (a_1) and 0.07 ± 0.01 and 0.16 ± 0.02 (a_2) in control and KN-93 respectively.

(C, D) Intracellular dialysis of cells with 1 μM KN-93 for 5 min did not change Kv1.5 currents recorded during 5 s depolarizations to +60 mV. Individual currents are shown in (C) and the diary of sustained current amplitude in (D). (E, F) Intracellular dialysis of cells with 1 μM KN-93 for 5 min did not change hERG currents recorded during 4 s depolarizations to +20 mV followed by 4 s pulses to –50 mV. Individual currents are shown in (E) and the diary of peak tail current amplitude in (F). NB, addition of 1 μM KN-93 to the bath solution (i.e. extracellularly) resulted in a rapid decline of both Kv1.5 and hERG currents.

Figure 5. Effect of KN93 on the rate of recovery from inactivation. Currents recorded (from the same cell) during a 5 s conditioning pulse to +60 mV to allow slow inactivation followed by brief 10 ms test pulses to +60 mV at different intervals to measure the recovery of channels from inactivation in control conditions (A) and with 1 μM KN-93 (B). (C) Peak test pulse current normalized to the peak conditioning pulse current plotted again pulse interval. Data were fitted to a double exponential function and the time constants (τ_{fast} and τ_{slow}) and the amplitudes (a_{fast} and a_{slow}) of each component are shown (n=5). *Significantly different (p<0.05) from control.

Figure 6. Mutants that accelerate or slow inactivation alter KN-93 block of Kv1.5. (A) Kv1.5 R487V currents recorded during 1 s depolarizing pulses to +60 mV from the holding potential of –80 mV in the absence and presence of KN-93. (B) A model of the outer pore of Kv1.5 based on the known crystal structure of Kv1.2 (accession: 2A79). The outer pore regions of only two subunits are shown for clarity. The side chains that were mutated are highlighted to show their position within the outer pore region. Spheres indicate K^+ ion coordination sites within the pore. (C) T462C currents recorded during 500 ms pulses to +60 mV from the holding potential of -80 mV in the absence and presence of increasing concentrations of KN-93 as indicated. (D) Concentration-response curve for KN-93 block of T462C mutant channels (n=4).

(E) Summary of the effect of KN-93 on each mutant tested. Bars show the fractional current remaining at the end of the pulse. *Significantly different ($p<0.05$) from wild-type Kv1.5. n.f. stands for non-expressing channels (n = 3-6).

Figure 1:

JPET Fast Forward. Published on December 20, 2005 as DOI: 10.1124/jpet.105.097618
This article has not been copyedited and formatted. The final version may differ from this version.

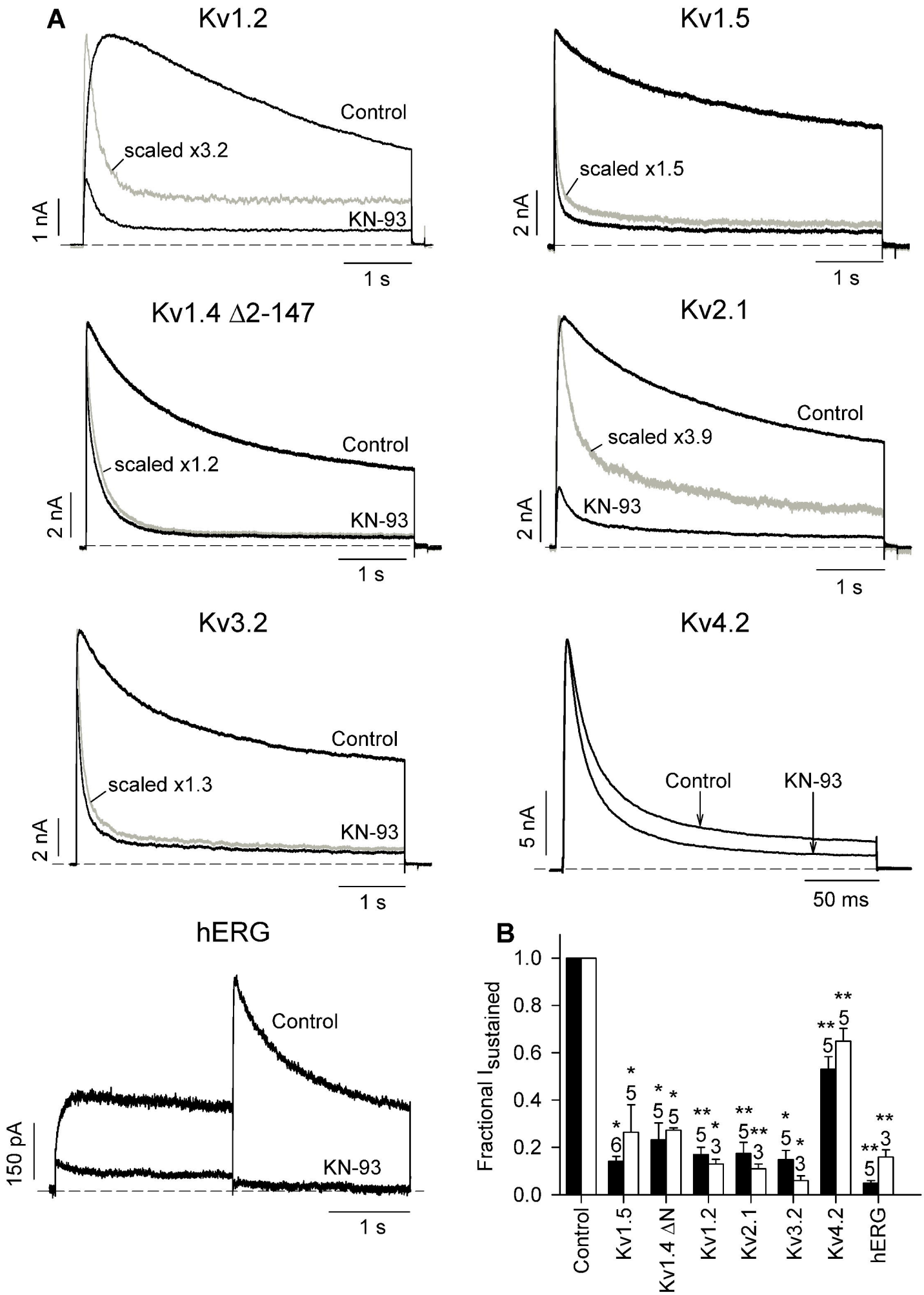

Figure 2:

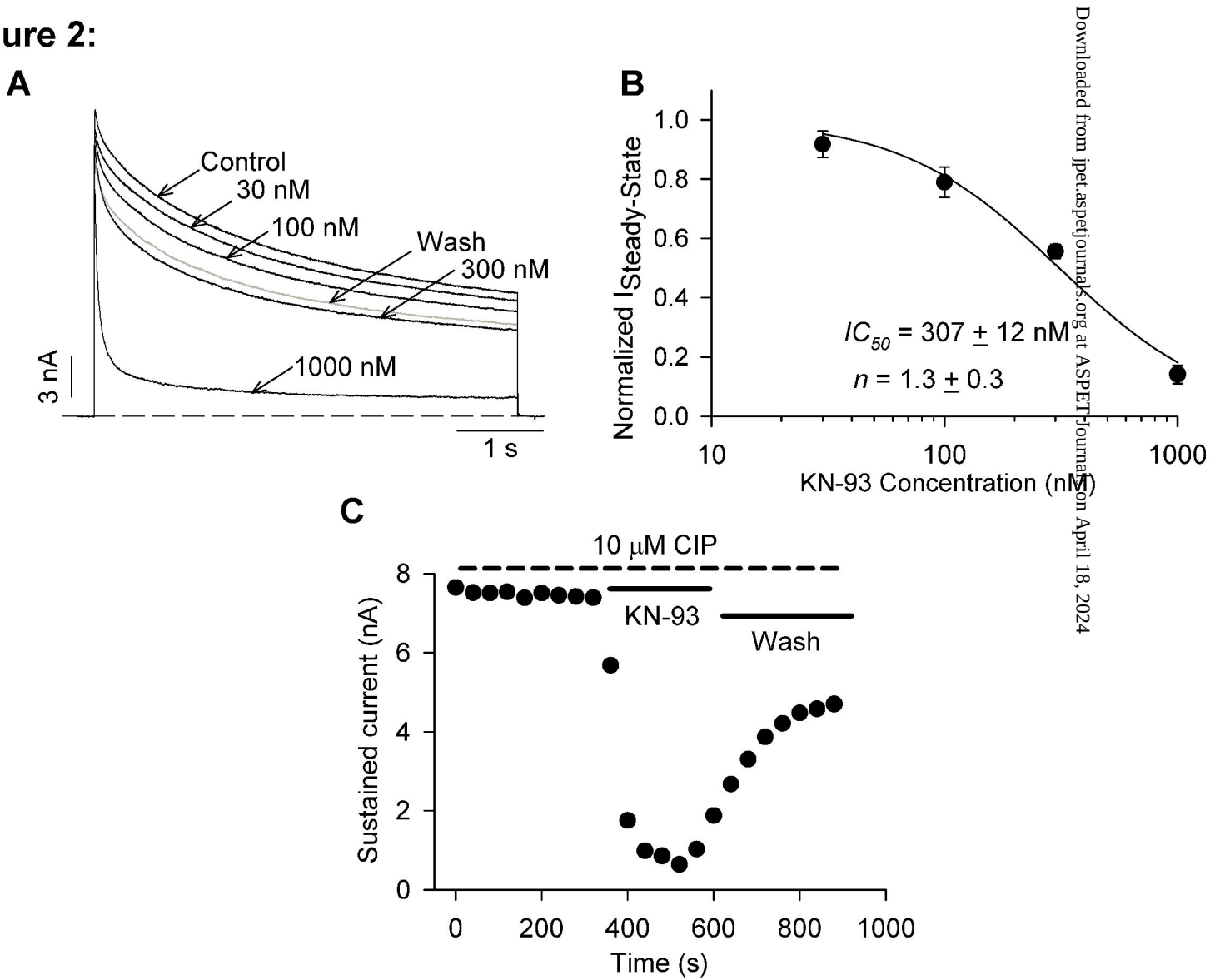

Figure 3:

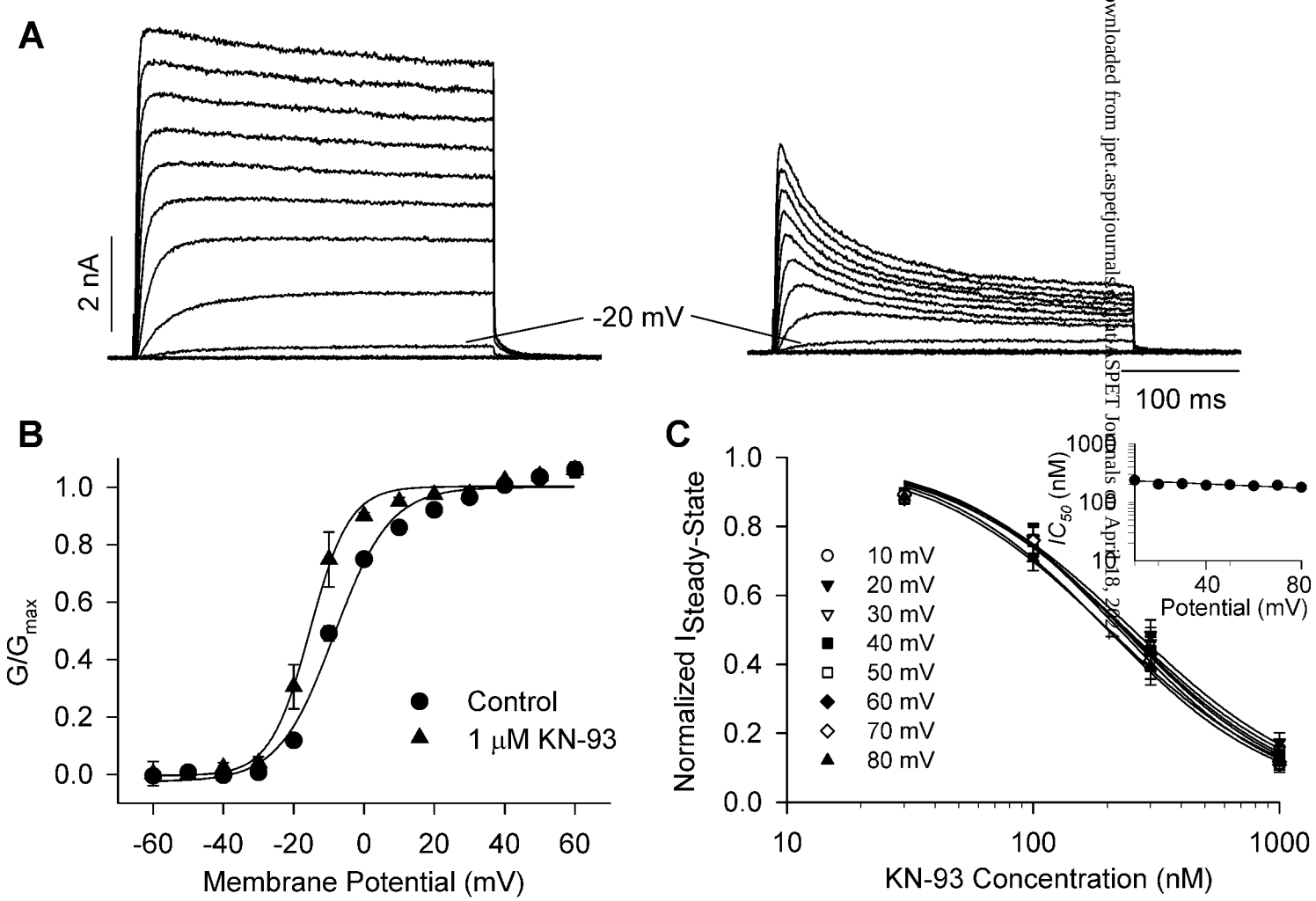

Figure 4:

JPET Fast Forward. Published on December 20, 2005 as DOI: 10.1124/jpet.105.097618
This article has not been copyedited and formatted. The final version may differ from this version.

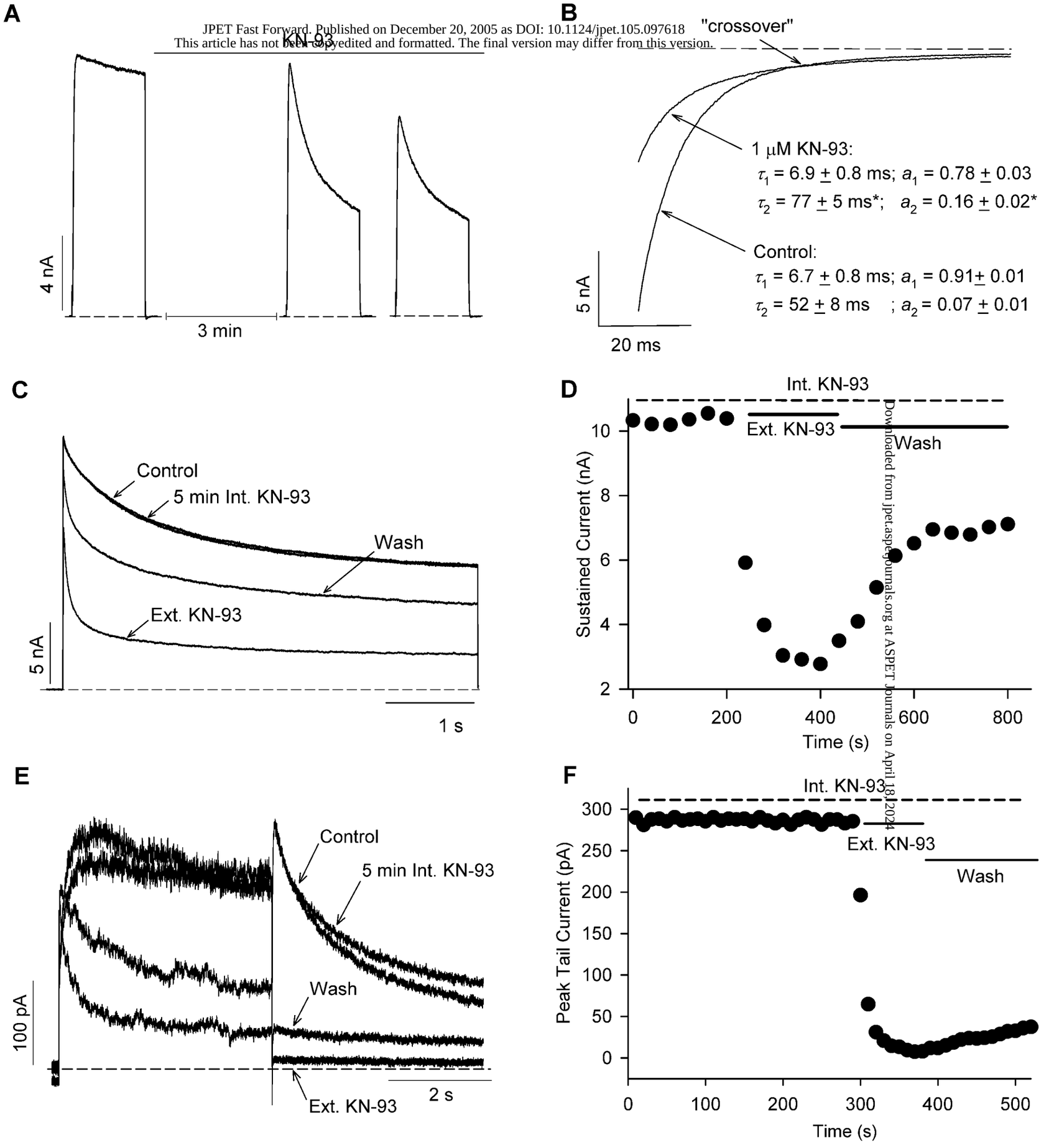

Figure 5:

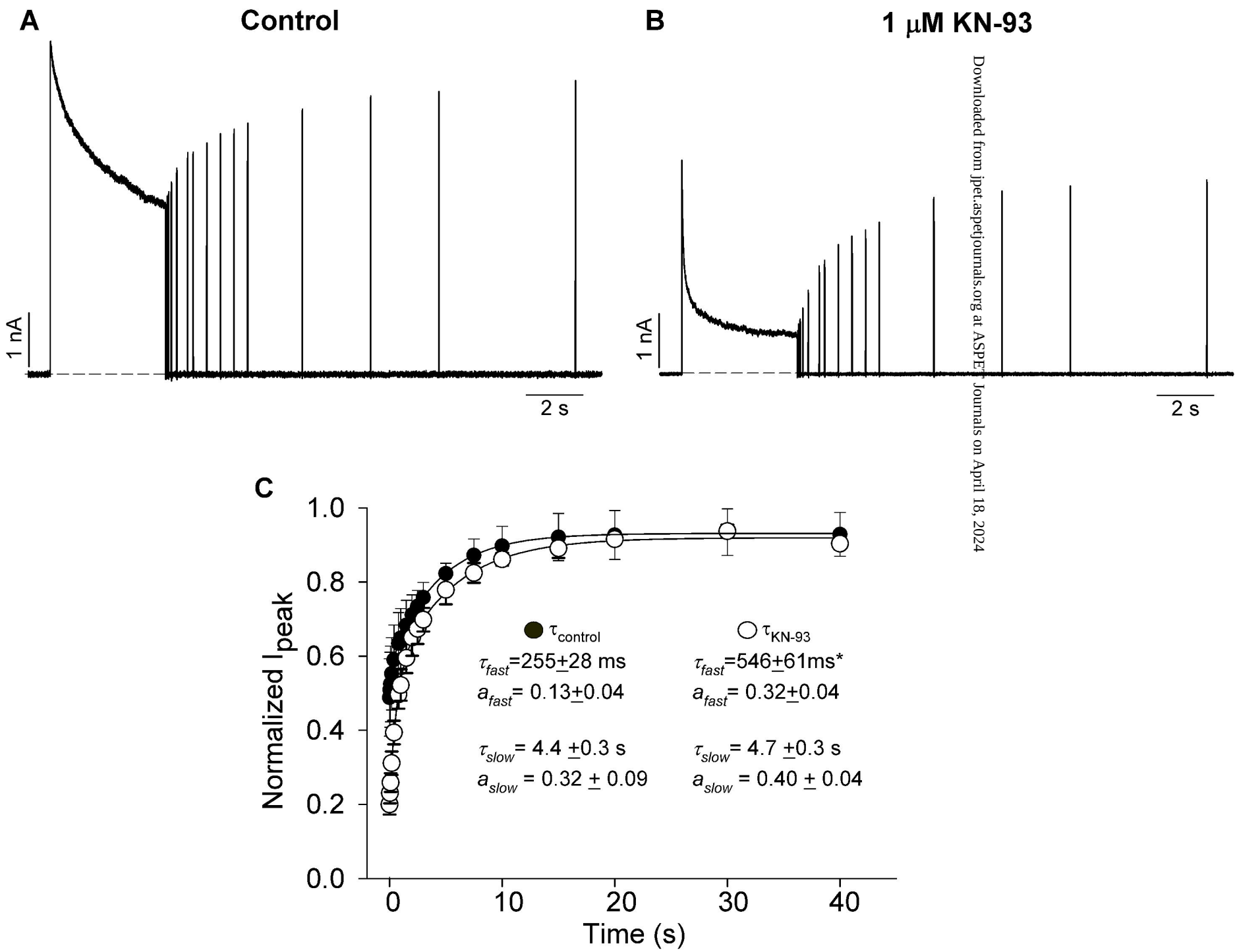

Figure 6: